Металлофиз. новейшие технол. / Metallofiz. Noveishie Tekhnol.
2015, т. 37, № 11, сс. 1549–1565
Оттиски доступны непосредственно от издателя
Фотокопирование разрешено только
в соответствии с лицензией

ДЕФЕКТЫ КРИСТАЛЛИЧЕСКОЙ РЕШЁТКИ

PACS numbers: 61.05.cp, 61.66.Dk, 62.20.de, 64.70.kd, 64.75.Bc, 81.30.Bx

Quantitative Methods for the Study of Al–Li Alloys: Phase Composition, Anisotropy of Properties, and Phase Stability

S. Betsofen, I. Grushin, M. Knyazev, and M. Dolgova

MATI—Russian State Technological University Named After K. E. Tsiolkovsky,
3 Orshanskaya Str.,
121552 Moscow, Russian Federation

A quantitative approach to the determination of the ratio between binary and ternary intermetallic phases in the Al–Mg(Cu)–Li alloys is developed on the basis of the balance equations of the chemical and phase compositions as well as the experimentally measured lattice parameter of the α-solid solution. As shown, for the Al–Mg(Cu)–Li alloys, the ratio between the fractions of the δ′ (Al_3Li) and S_1 (T_1) phases is determined by the ratio between the molar fractions of Li and Mg (Cu). The equations for the calculation of the contents of the S_1 (Al_2MgLi), T_1 (Al_2CuLi) and δ′ (Al_3Li) phases in the 1420, 1424, 5090 alloys (Al–Mg–Li alloys) and in the 1440, 1460, 1461, 1441, 1469, 2090, 2094, 2095, 8090, Weldalite 049 alloys (Al–Cu–Li alloys) used in Russia and other countries are given. The possibilities of the method application for the study and prediction of the phase stability and anisotropy of the elastic and strength properties are considered.

Key words: Al–Mg–Li and Al–Cu–Li alloys, intermetallic compounds, lattice parameter, quantitative phase analysis, anisotropy, phase stability.

Розроблено кількісний підхід для визначення співвідношення бінарних і трикомпонентних інтерметалевих фаз у стопах Al–Mg(Cu)–Li, заснований на рівняннях рівноваги хемічних і фазових складів, а також експериментально виміряній сталій кристалічної ґратниці α-твердого розчину. Показано, що для стопів Al–Mg(Cu)–Li співвідношення між фракціями фаз δ′ (Al_3Li) і S_1 (T_1) визначаються співвідношенням між мольними частками Li і Mg (Cu). Наведено рівняння для розрахунку вмісту фаз S_1

Correspondence author: Sergej Yakovlevich Betsofen
E-mail: s.betsofen@gmail.com

S. Betsofen, I. Grushin, M. Knyazev, and M. Dolgova,
Quantitative Methods for the Study of Al–Li Alloys: Phase Composition, Anisotropy of Properties, and Phase Stability, *Metallofiz. Noveishie Tekhnol.*, **37**, No. 11: 1549–1565 (2015).

(Al_2MgLi), T_1 (Al_2CuLi) і δ' (Al_3Li) у стопах 1420, 1424, 5090 (стопи Al–Mg–Li) та у стопах 1440, 1460, 1461, 1441, 1469, 2090, 2094, 2095, 8090, Weldalite 049 (стопи Al–Cu–Li). Розглянуто можливості застосування цієї методи для вивчення та передбачення фазової стабільности й анізотропії пружніх і міцнісних властивостей.

Ключові слова: стопи Al–Mg–Li і Al–Cu–Li, інтерметалічні з'єднання, параметр ґратниці, кількісний фазовий аналіз, анізотропія, фазова стабільність.

Разработан количественный подход для определения соотношения бинарных и трёхкомпонентных интерметаллических фаз в сплавах Al–Mg(Cu)–Li, основанный на уравнениях равновесия химических и фазовых составов, а также экспериментально измеренной постоянной кристаллической решётки α-твёрдого раствора. Показано, что для сплавов Al–Mg(Cu)–Li соотношение между фракциями фаз δ' (Al_3Li) и S_1 (T_1) определяется соотношением между мольными долями Li и Mg (Cu). Приведены уравнения для расчёта содержания фаз S_1 (Al_2MgLi), T_1 (Al_2CuLi) и δ' (Al_3Li) в сплавах 1420, 1424, 5090 (сплавы Al–Mg–Li) и в сплавах 1440, 1460, 1461, 1441, 1469, 2090, 2094, 2095, 8090, Weldalite 049 (сплавы Al–Cu–Li). Рассмотрены возможности применения данного метода для изучения и предсказания фазовой стабильности и анизотропии упругих и прочностных свойств.

Ключевые слова: сплавы Al–Mg–Li и Al–Cu–Li, интерметаллические соединения, параметр решётки, количественный фазовый анализ, анизотропия, фазовая стабильность.

(Received October 7, 2015)

1. INTRODUCTION

Significant progress in the use of new materials in aviation industry is associated with composite materials such as Glass Laminate Aluminium Reinforced Epoxy (GLARE). In contrast to one-layer sheets of aluminium alloys, such composite materials are characterized by decreased density (by 10–15%), high strength, low fatigue crack propagation rate, and fire resistance. The application of GLARE for the fuselage skin of the A-380 Airbus results in a weight saving of more than 500 kg. A new research work aimed at the development of a new generation of GLARE -based Al–Cu–Li alloys in VIAM would increase the modulus of elasticity by 8–10% and reduce the density by 5–7% [1, 2]. Despite all these advantages, the Al–Li alloys are not used widely enough, mainly because of their low thermal stability, which manifests itself in a reduction in ductility and fracture toughness upon long-term low-temperature heating (LLH), low deformability (small reductions per unit pass upon cold rolling), and severe anisotropy of mechanical properties [3].

It has been established that the problem of LLH is caused by the precipitation of the δ′-phase and by the resulting structure defects [4]. A decrease in lithium concentration in the alloy reduces the severity of the problem but does not solve it entirely, because the δ′-phase precipitation process is tightly connected with the other phases in the alloy (T_1, θ′) and, therefore, with the copper content in the alloy. In addition, a decrease in the lithium content would reduce the elastic and strength properties. It is also known that the anisotropy of mechanical properties in aluminium alloys is definitely related to the crystallographic texture [5, 6]. However, it is not clear, why this problem is significantly more pronounced in the lithium-containing alloys, which do not differ from other aluminium alloys in texture. This can be explained only by the fact that the alloys with lithium are characterized by a high content of intermetallic phase, which differs from the aluminium matrix in the anisotropy of properties.

In general, the aim of optimizing the composition and production technology of semi-finished sheets and their heat treatment comes to establishing the quantitative correlations of main alloying elements in the alloy and heat treatment with the quantitative ratio between the major strengthening intermetallic phases. This task is addressed in the work.

2. MATERIALS AND EXPERIMENTAL METHODS

To design a quantitative X-ray diffraction analysis technique, we used commercial Al–Mg–Li alloy grade 1420 (5.6 Mg, 2.0 Li, 0.3 Mn, 0.1Zr, Al for balance) and Al–Cu–Li alloy grade V-1461 (Al–2.8Cu–1.7Li–0.5Mg–0.5Zn–0.1Zr–0.06Sc). X-ray diffraction analysis was performed on a DRON-4.0 diffractometer using filtered CuK_α-radiation and (333)/(511) reflections of the α solid solution which have a Bragg angle approaching 80° in order to obtain a high accuracy in lattice parameter measurement.

The basic equations for calculating the changes in volume and linear dimensions of the aluminium alloys are given in [7–9]. The lattice parameters of the solid solution (a_α) for binary aluminium alloys, in accordance with Végard's law, is linearly related to the content of the i-th alloying element (X_i):

$$a_\alpha = a_{\mathrm{Al}} + \left(\frac{\Delta a}{\Delta X}\right)_i^\alpha X_i, \qquad (1)$$

where $\left(\frac{\Delta a}{\Delta X}\right)_i^\alpha$ is the change in the lattice parameter per 1 weight percent of the alloying element, Å/wt.%.

Table 1 shows the data on $\left(\frac{\Delta a}{\Delta X}\right)_i^{\alpha}$, compositions, and specific volumes of intermetallic phases in the Al–Mg, Al–Cu, Al–Mg–Li, and Al–Cu–Li alloys.

The information on the quantitative relationships of phases in the alloys can reliably control the state of the alloys after deformation and heat treatment. Furthermore, knowing the phase composition, one can calculate the volume and linear dimensional changes accompanying heat treatment.

The specific volume of the mixture can be calculated using the specific volumes of the phases and their weight percentages by the rule of mixtures:

$$V_m = \frac{W_A V_A + W_B V_B}{100}, \qquad (2)$$

where W_A is the weight percentage of the A phase; V_A is the specific volume of the A phase; W_B is the weight percentage of the B phase; and V_B is the specific volume of the B phase, *etc*.

Substituting the weight percentages of phases into Eq. (2), we obtain the volume effects for phase precipitation in binary alloys. The necessary data on the precipitate density or specific volume can be calculated on the basis of the composition and crystal structure of such phases. The data for the determination of the phase composition of the Al–Mg–Li alloys are given in [8]. The same approach can be used for the Al–Cu–Li alloys [9]:

TABLE 1. Data for the calculation of the phase compositions of the Al–Mg, Al–Cu, Al–Mg–Li, and Al–Cu–Li alloys (a_{Al} = 4.0493·10^{-8} cm, A_{Al} = 26.98 g/mole, $V_{Al} = 1/\rho_{Al}$ = 0.3705 cm^3/g, and Y is the content of alloying element in at.%).

Element	$\left(\frac{\Delta a}{\Delta X}\right)_i^{\alpha} \cdot 10^3$	$\left(\frac{\Delta a}{\Delta Y}\right)_i^{\alpha} \cdot 10^3$	Phase	Concentration of alloying elements X	Specific volume V_B
	Å/wt.%	Å/at.%		wt.%	cm^3/g
Al (balance)	–	–	–	–	0.3705
Mg	+5.18	+4.62	β (Al_3Mg_2)	37.6	0.448
			Θ′ (Al_2Cu)	54.2	0.2472
Li	–	–	AlLi	20.5	0.5744
			Al_3Li	7.9	0.4583
Cu + Li	–	–	T_1 (Al_2CuLi)	5.5Li–51.1Cu	0.3223
Mg + Li	–	–	S_1 (Al_2MgLi)	8.1Li–28.5Mg	0.5602

$$W_\alpha = \frac{(X^\delta_{Li} - X^{T_1}_{Li})(X^0_{Al}X^{T_1}_{Cu} - X^{T_1}_{Al}X^0_{Cu}) - X^\delta_{Al}X^{T_1}_{Cu}(X^0_{Li} - X^{T_1}_{Li})}{(X^\delta_{Li} - X^{T_1}_{Li})(100X^{T_1}_{Cu} - X^\alpha_{Cu}X^{T_1}_{Cu} - X^{T_1}_{Cu}X^\alpha_{Li} - X^{T_1}_{Al}X^\alpha_{Cu}) - X^\delta_{Al}X^{T_1}_{Cu}(X^\alpha_{Li} - X^{T_1}_{Li})} \times 100,$$

$$W_{T_1} = \frac{100X^0_{Cu} - X^\alpha_{Cu}W_\alpha}{X^{T_1}_{Cu}}, \quad (3)$$

$$W_{\delta'} = 100 - W_\alpha - W_{T_1},$$

where X^0_{Al}, X^0_{Cu}, and X^0_{Li} are the Al, Cu, and Li concentrations in the alloy, respectively (wt.%), W_α, W_{T_1}, and $W_{\delta'}$ are the weight percentages of the α, T_1, and δ′ phases, respectively, and X^α_{Al}, X^α_{Cu}, X^α_{Li}, $X^{T_1}_{Al}$, $X^{T_1}_{Li}$, $X^{T_1}_{Cu}$, $X^{\delta'}_{Al}$, and $X^{\delta'}_{Li}$ are the Al, Cu, and Li concentrations in the α-, T_1-, and δ′-phases, respectively. The $X^{S_1}_{Al}$, $X^{\delta'}_{Al}$, $X^{T_1}_{Al}$, $X^{T_1}_{Li}$, and $X^{\delta'}_{Li}$ parameters are calculated from the stoichiometry of the T_1 (Al_2CuLi) and δ′ (Al_3Li) phases. These data are given in Table 1. The X^α_{Cu} parameter is determined from the lattice parameter of the solid solution (a_α). Eq. (3) allows one to determine the ratio between the α-, T_1- and δ′-phases for each lithium content in the α-phase (X^α_{Li}).

3. RESULTS AND DISCUSSION

3.1. Quantitative Phase Analysis (QPA) of the Al–Li Alloys

Figures 1 and 2 show the contents of intermetallic phases for the 1420 and V-1461 alloys. In the calculations, the lithium concentration in the solid solution was taken to be 0.5%, which corresponds to the δ′-phase content realized after long-term natural aging for the alloys. Figure 1 shows that, for the Al–Cu–Li alloys, the δ′-phase content is much higher than the T_1-phase content. In this case, the ratio between them is determined by the ratio between the lithium and copper concentrations in the alloy. Indeed, the maximum T_1-phase content corresponds to the absence of copper in the solid solution and, in this case, is determined by the molar concentration of copper in the alloy. The maximum δ′-phase content corresponds to the absence of lithium in the solid solution and is also determined by the difference between the lithium and copper molar concentrations, since the composition of the ternary phase is Al_2CuLi, and, in the case where the solid solution contains neither copper nor lithium, these elements are forced to be distributed between these intermetallics. By the way, the formation of certain amounts of the Θ (Θ′, Θ″) phases only decreases the T_1-phase content at the expense of the binary phase precipitation. Since copper is contained only in the ternary phase, in which each copper atom falls on a lithium atom, the difference in the molar concentrations of copper and lithium regulates the maximum δ′-phase content in the alloy.

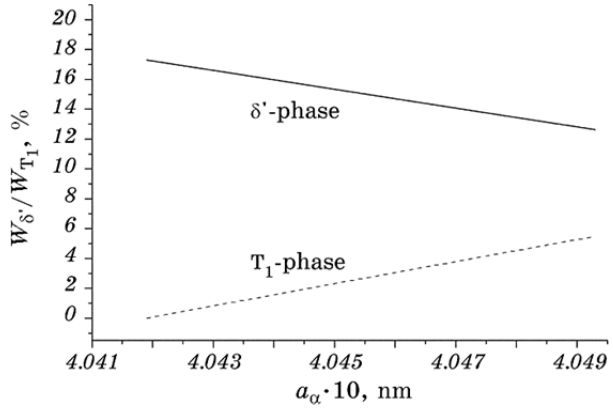

Fig. 1. Ratio between the δ′ (solid line) and T_1 (dashed line) intermetallic phases in the V-1461 as a function of the lattice parameter of the solid solution (a_α) for lithium contents in the solid solution (X^α_{Li}) of 0.5% .

If we compare the phase relationships between the δ′-phase and the ternary phases in the Al–Cu–Li (Fig. 1) and Al–Mg–Li (Fig. 2) alloys, we clearly see that their contents in the alloys with magnesium are about the same, while the δ′-phase content in the Al–Cu–Li alloys substantially exceeds the content of the ternary phase. As was mentioned above, the ratio between the contents of the δ′ (Al_3Li) and S_1 (T_1) phases is determined by the ratio between the molar concentrations of Li and Mg (Cu). In the Al–Mg–Li alloys, the ratio between the Li and Mg molar fractions is 1.0–1.5, and therefore, the contents of the δ′- and S_1-phases are approximately the same, while, in the Al–Cu–Li alloys, the

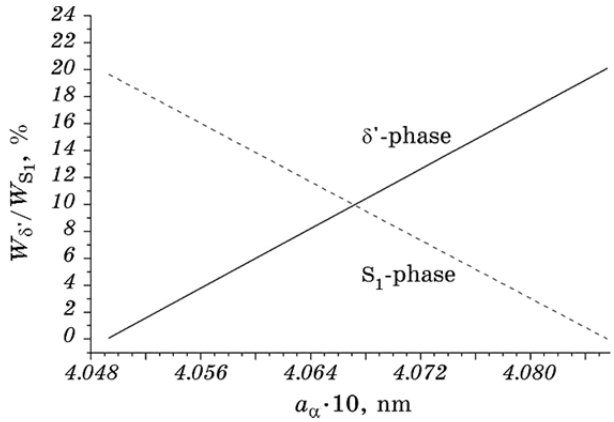

Fig. 2. Ratio between the δ′ (solid line) and S_1 (dashed line) intermetallic phases in the 1420 alloy as a function of the lattice parameter of the solid solution (a_α) for lithium contents in the solid solution (X^α_{Li}) of 0.5% .

ratio between the Li and Cu molar fractions ranges from 2 to 19, and therefore the δ′-phase dominates.

3.2. Anisotropy of Mechanical Properties

Many intermetallic phases, especially δ′-phase in the lithium-containing alloys, are responsible for the unusual strength anisotropy, which in the textured sheets from these alloys [5, 6] substantially exceeds the anisotropy of the properties of other aluminium alloys with virtually similar textures. This anisotropy can be due to the precipitation of the textured δ′-phase upon rolling.

To explain this effect, one should analyse the effect of the $L1_2$ type ordered δ′-phase on the anisotropy of mechanical properties in the lithium-containing alloys. This phase is characterized by a texture, which is similar to the texture of the solid solution [6], but, at the same time, has a specific deformation mechanism caused by the long-range ordering. The $L1_2$-type ordered δ′-phase radically differs from the solid solution in the character of the orientation dependence of shear stress. For example, the maximum and minimum strength of the solid solution corresponds to the <111> and <100> directions, respectively.

By contrast, the maximum strength of the $L1_2$-ordered structures corresponds to the <100> direction as for the single crystals of nickel superalloys, since, for this direction, the Schmid factor for slip over the {001}<110> system is zero. For the $L1_2$-type ordered structures, slip in the cube planes at high stacking fault energy (SFE) may be more favourable than in the close-packed planes, because the slip in the former case is less out of order. Considering this, the authors of [6] proposed a simple calculation procedure for evaluating the yield strength anisotropy in the Al–Li alloys containing the ordered phase with the $L1_2$ lattice in addition to the FCC solid solution. The yield stress anisotropy in the sheet directions (RD, TD, and 45° to RD) was proposed to be estimated by the ratio between the Zacks factors, M, calculated on the basis of the texture data. In this case, the calculation relationships allow for the difference in the critical resolved shear stress for the δ′- and α-phases:

$$\sigma_{0.2}{}^{\mathrm{RD}}/\sigma_{0.2}{}^{45} = \mathrm{M}_{\mathrm{alloy}}{}^{\mathrm{RD}}/\mathrm{M}_{\mathrm{alloy}}{}^{45}, \quad \sigma_{0.2}{}^{\mathrm{TD}}/\sigma_{0.2}{}^{45} = \mathrm{M}_{\mathrm{alloy}}{}^{\mathrm{TD}}/\mathrm{M}_{\mathrm{alloy}}{}^{45}$$

$$\mathrm{M}_{\mathrm{alloy}}{}^{(\mathrm{RD,\ 45,\ TD})} = \beta \mathrm{M}_{\delta'}{}^{(\mathrm{RD,\ 45,\ TD})} V_{\delta'} + (1 - V_{\delta'}) \mathrm{M}_{\alpha}{}^{(\mathrm{RD,\ 45,\ TD})},$$

where $\beta = \tau_{\delta'}{}^{\{001\}<110>}/\tau_{\alpha}{}^{\{111\}<110>}$ is ratio between the critical resolved shear stress for slip over the {001}<110> system of the δ′-phase and slip over the {111}<110> system of the α-phase,

$$\mathrm{M}_{\delta'}{}^{(\mathrm{RD,45,TD})} = [\Sigma(\alpha^{-1}\Phi_{\delta'}{}^{\{111\}<110>}\mathrm{P}_{\alpha})_{hkl} + \Sigma(\Phi_{\delta'}{}^{\{001\}<110>}\mathrm{P}_{\alpha})_{hkl}]^{-1},$$

$$M_{\alpha}^{(RD,45,TD)} = [\Sigma(\Phi_{\alpha}^{\{111\}<110>} P_{\alpha})_{hkl}]^{-1},$$

$\alpha = \tau_{\delta'}^{\{111\}<110>} / \tau_{\delta'}^{\{001\}<110>}$ is the ratio between the critical resolved shear stress for slip over the {111}<110> and {001}<110> systems of the δ′-phase, and $V_{\delta'}$ is the volume fraction of the δ′-phase.

The results of the calculation of the yield strength anisotropy show that, varying the α and β parameters, one can widely change the calculated anisotropy at the same phase ratios and texture. The agreement between the calculated and experimental anisotropy parameters is achieved at α = 2.8 and β = 6. Thus, the anisotropy of the mechanical properties of the lithium-containing alloys substantially depends on the δ′-phase content and orientation. This explains the well-known fact that heat treatment radically changes the anisotropy, but retains the texture of the solid solution virtually unchanged [5] because, in this case, the δ′-phase of deformation origin is dissolved, and the δ′-phase precipitating upon cooling has a different texture even if its nucleation is oriented due to the realization of various transformation versions.

3.3. Elastic Properties

In addition to significant advantage in weight characteristics, the application of the Al–Li alloys for components of GLARE is based on the fact that Young's modulus of the lithium-containing alloys is substantially higher than that of other aluminium alloys. It was shown [12] that an increase in GLARE Young's modulus at the expense of the metal component is much more effective than increased Young's modulus of prepreg.

There are two ways to increase the elastic modulus of metal alloys. The first method is based on the anisotropy of Young's modulus and the possibility to use the favourable texture of the sheet to increase the Young's modulus in its plane. The second method of increase in the elastic modulus is the formation of intermetallic phase particles, which in the alloy typically have higher elastic properties than the matrix. As was shown in [13], the highest Young's modulus (82.6 GPa) of the 8090 alloy (Al–2.4Li–1.14Cu–0.67Mg) was exhibited by the sample with a high δ′-phase content.

The magnitude of the elastic moduli of crystals with cubic lattice is calculated by the following formula:

$$1/E_{hkl} = S_{11} - 2J\Gamma,$$

where $J = S_{11} - S_{12} - 0{,}5S_{44}$ ($J > 0$ is the positive anisotropy, $J < 0$ is the negative anisotropy), and $\Gamma = (h^2k^2 + h^2l^2 + k^2l^2)/(h^2 + k^2 + l^2l^2)^2$ is the orientation factor.

Table 2 shows Young's moduli for different crystallographic directions in Al and Cu. The anisotropy of the elastic properties of aluminium is small; the difference between the maximum (<111>) and minimum (<100>) Young's moduli does not exceed 20%. This value is very small, with allowance for the fact that Table 2 shows the moduli for single-crystal orientations. In the case of even highly textured polycrystalline metal, this difference will decrease at least by a factor of two. To demonstrate that small anisotropy is not characteristic of all metals with cubic lattice, Table 2 represents Young's moduli for different orientations of copper, for which this difference is almost threefold.

Table 3 shows Young's moduli for different directions in aluminium sheets for the texture components typical of aluminium. It is seen that the anisotropy of the elastic moduli for aluminium is not a sufficiently effective way to increase the elastic properties since the maximum modulus in the <111> direction is only 76 GPa. Therefore, increased Young's modulus in the lithium containing alloys can be explained only by a substantial content of the ordered δ′-phase. To obtain Young's modulus of 80–82 GPa characteristic of the lithium-containing alloys, it is sufficient to have ≅ 20% δ′-phase with a Young's modulus of 115–

TABLE 2. Young's moduli for various directions in Al and Cu.

uvw	*E*, GPa	
	Al	Cu
111	76.1	191.6
110	72.6	130.5
112	72.6	130.5
113	69.0	96.3
100	63.7	66.8
Average	70.7	121.8

TABLE 3. Anisotropy of Young's moduli for various texture components of Al sheets.

Texture	ND		RD		TD	
	[*uvw*]	*E*, GPa	[*uvw*]	*E*, GPa	[*uvw*]	*E*, GPa
{112}<11 $\bar{1}$ > 'TCu'	112	72.6	11 $\bar{1}$	76.1	112	72.6
{011}<21 $\bar{1}$ > 'TBr'	011	72.6	21 $\bar{1}$	72.6	1 $\bar{1}$ 1	76.1
{001}<110> 'TC'	001	63.7	110	72.6	$\bar{1}$ 10	72.6
{110}<001> (TG)	110	72.6	001	63.7	$\bar{1}$ 10	72.6

120 GPa, which is realistic.

3.4. Thermal Stability

The determination of the quantitative phase composition of the Al–Mg(Cu)–Li alloys allows one to predict their important properties such as thermal stability and elastic moduli. Figure 3 shows the scheme for the calculation of such parameters as a function of the alloy composition. The parameter of thermal stability can be taken as $W_{\delta'}^{\max}$, which is the difference between the maximum and minimum δ′-phase contents at two fixed lithium contents in the α solid solution. This parameter shows the quantity of the δ′-phase, which can precipitate from the solid solution maximally supersaturated with lithium (maximum lithium concentration) until its complete withdrawal from the solid solution (zero concentration). Since we need the value of this parameter, which allows us to compare alloys with different contents of alloying elements, we can take an arbitrary value close to the maximum solubility of lithium in solid solution. Figure 3 shows the scheme for a lithium content of 0.5%, but with the same success, we can take 0.7 or 0.9%. This is no matter for comparative evaluation of the thermal stability of the alloys.

The level of elastic properties depends on the δ′-phase content in the alloy, so the maximum content ($W_{\delta'}^{\max}$), which can be calculated for a given Al–Mg(Cu)–Li alloy composition (Fig. 3), is a quantitative characteristic of its Young's modulus. The 8090 alloy (Fig. 3, *a*) is characterized by low $\Delta W_{\delta'}^{\max}$, which indicates a high phase stability of this alloy since, at all thermomechanical actions, no more than 6.3% δ′-phase, which is about 20% of its maximum quantity, can precipitate from the solid solution. At the same time, $\Delta W_{\delta'}^{\max}$ of the Weldalite 049 alloy (Fig. 3, *b*) is almost three times higher (15.9%), which indicates, on the one hand, its phase instability, and, on the other hand, the possibility to vary its structural and phase state in a wide range. This gives a great opportunity to correct the complex of the properties of welded joints, for which this alloy is used successfully. The 8090 alloy should have high elastic properties, since the δ′-phase content in it can reach 30% (Fig. 3, *a*). This substantially differentiates the 8090 alloy from the Weldalite 049 alloy with much smaller δ′-phase content (Fig. 5, *b*). Figures 4 and 5 shows the corresponding quantitative parameters, on the basis of which one can search for alloys, depending on the necessary combinations of service properties.

It is seen that the Al–Mg–Li alloys substantially differ from the Al–Cu–Li alloys in the combination of the characteristics including the parameters of phase stability and elastic properties. The Al–Mg–Li alloys (Fig. 4, *a*) are characterized by high phase instability, even in comparison with the most instable alloys of the Al–Cu–Li system (the

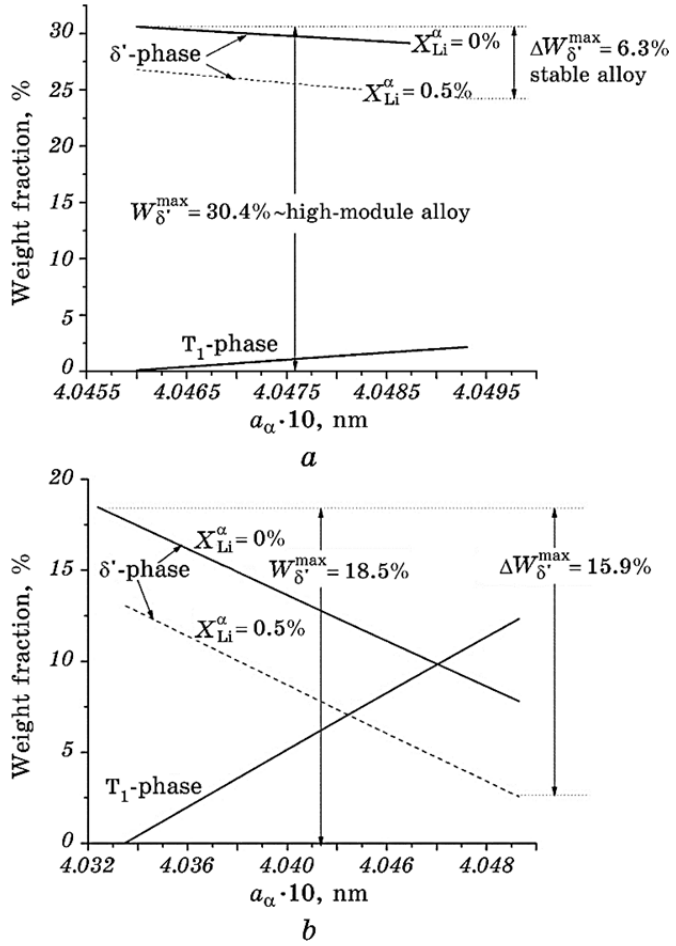

Fig. 3. Scheme of the determination of the Al–Li–Cu alloy thermal instability parameter, which characterizes the resistance to instability upon long-term low-temperature heatings: the 8090 (Al–1.1Cu–2.4Li) (*a*) and Weldalite 049 (Al–6.3Cu–1.3Li) alloys: $\Delta W^{max}_{\delta'}$ is the maximum δ′-phase content in the alloy; $\Delta W^{max}_{\delta'}$ is the thermal instability parameter equal to the maximum possible quantity of the δ′-phase, which can be precipitated from the solid solution (*b*).

American Weldalite 049 alloy and the Russian 1460-3 alloy; see. Fig. 5, *b*). The most thermally stable alloys of the Al–Cu–Li system (Fig. 4, *b*) considerably surpass the Al–Mg–Li alloys (Fig. 4, *a*) in this parameter.

The data on the quantities of intermetallic phases precipitating from the solid solution upon heat treatment and deformation of the Al–Mg–Li alloys can be used for the estimation of the volume changes

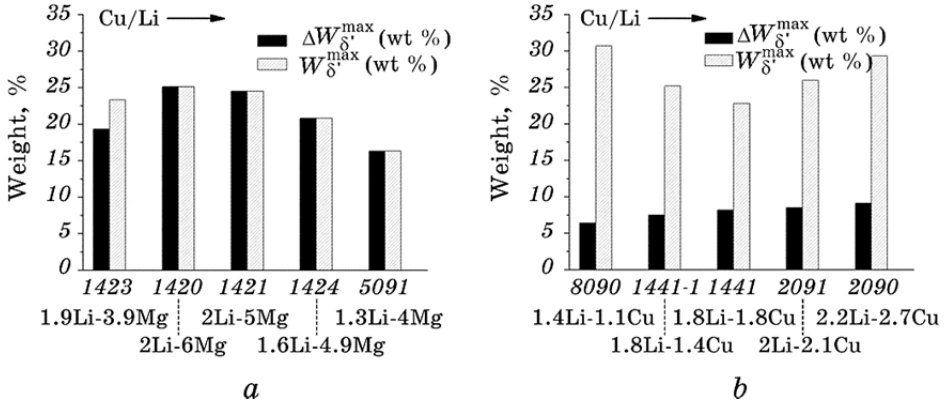

Fig. 4. Thermal instability parameter and δ′-phase content for the commercial Al–Mg(Cu)–Li alloys: the Al–Mg–Li alloys with a high level of thermal instability (high $W_{\delta'}^{max}$) and a high δ′-phase content (high $W_{\delta'}^{max}$) (*a*) and the Al–Cu–Li alloys with a high thermal stability (low $\Delta W_{\delta'}^{max}$), and a high δ′-phase content (*b*).

upon the phase precipitation by Eqs. (2), (3). Figure 6 shows the volume effects calculated for the precipitation of some intermetallic phases in aluminium alloys per one volume percent of the precipitated phase.

Still higher volume effects are characteristic of the ternary phases (T_1, S_1), especially in the Al–Cu–Li alloys. The ternary phase (T_1) precipitation in these alloys is characterized by a very high positive volume effect (Fig. 6), which can lead to considerable internal stresses and

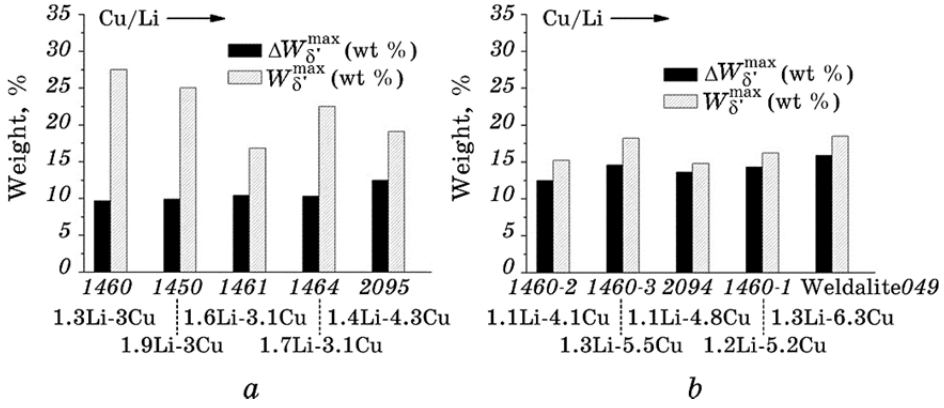

Fig. 5. Thermal instability parameter and δ′-phase content for the commercial Al–Cu–Li alloys: the alloys with a moderate level of thermal instability and a moderate δ′-phase content (*a*) and the alloys with a low thermal stability (high $\Delta W_{\delta'}^{max}$) and a low δ′-phase content (*b*).

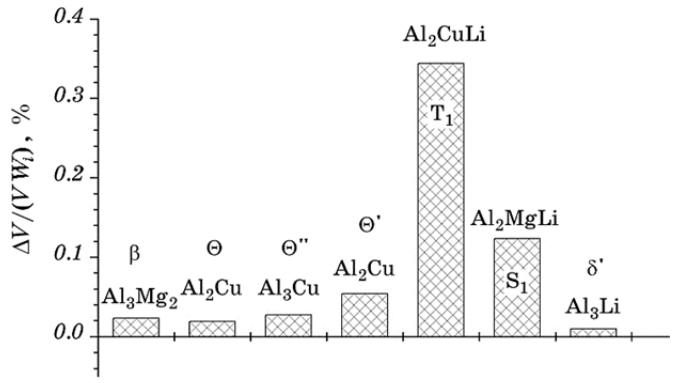

Fig. 6. Calculated volume effects of the aluminide precipitation from the solid solution per one percent of the precipitated phase (W_i is the amount of intermetallic phase).

related negative consequences for the manufacture of articles by edge cutting machining from thick semi-finished sections. In this case, a non-uniformity of the decomposition over the cross section can lead to the gradient of one-sign stresses from the centre of the plate to its periphery. This stress gradient can be accumulated upon removal of the surface layers and lead to strong deformation of the articles. On the other hand, a significant volume effect in combination with the fact that the ternary phase fraction in the Al–Cu–Li alloys is significantly lower than that is in the Al–Mg–Li alloys (see. Figs. 1, 2) allows one to minimize the precipitation of ternary phase in the Al–Cu–Li alloys. This is possible only through careful control of the mechanism of solid solution decomposition. Therefore, the proposed method of phase analysis is of practical importance for the optimization of the entire set of technological operations used for the manufacture of such alloys.

3.5. Effect of Lithium Solubility in Solid Solution (X_{Li}^{α}) on the QPA Accuracy

Lattice parameter varies within certain limits for each alloy composition and lithium content in the solid solution. The lowest and highest lattice parameters correspond to the maximum possible S_1-phase content and the maximum δ′-phase content, respectively. It should be emphasized that the developed technique is based on a formal assessment of the quantity of intermetallic phase on the basis of the chemical composition of the alloy and the lattice parameter of the solid solution and is not associated with the actual physical-chemical alloy characteristics defining, *e.g.*, the concentration of lithium in solid solution after

various regimes of heat or thermomechanical treatment. Nevertheless, the estimation of the quantitative ratio between phases allows an objective interpretation of the results of experimental metallographic studies and allows one to select the optimal regimes of these studies.

As an example, we consider the change in the phase composition of the 1420 alloy upon cold rolling (Fig. 7). With increasing degree of reduction of warm-rolled sheet, the lattice parameter of the solid solution decreases from 4.075 Å to 4.061 Å (Fig. 7, *a*). Table 4 shows the phase compositions calculated for different lithium compositions in the solid solution after deformation of the alloy to different degrees.

Various versions of changes in these parameters with increasing degree of reduction are considered with allowance for the fact that, upon cold rolling, the weight fraction of intermetallic phases cannot decrease, and the lithium content cannot correspondingly increase, *i.e.*, the phases only precipitate, but do not dissolve. This condition is quite realistic for cold rolling. The analysis of different 'routes' of the

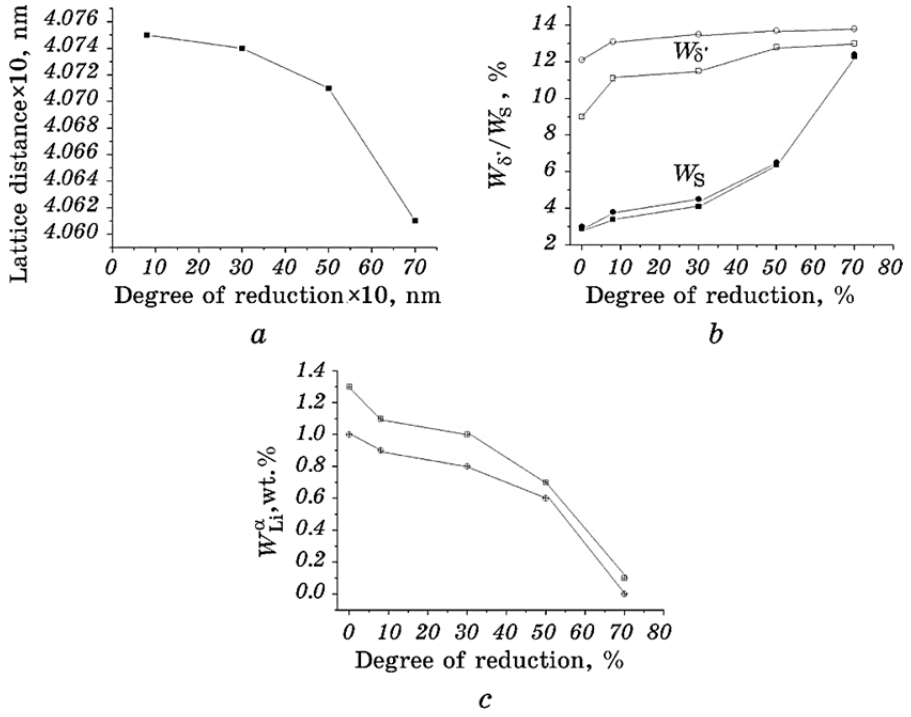

Fig. 7. Lattice parameter of the α-solid solution (*a*), calculated lithium concentration in the α-phase (*b*), and calculated contents of S_1- and δ′-phases (*c*) as a function of degree of reduction upon cold rolling of the 1420 alloy: the contents of phases ($W_{\delta'}$ and W_{S_1}) and the lithium concentration (X^{α}_{Li}) are given for the 1st and 2nd 'routes' identified in Table 4.

TABLE 4. Phase composition (W_{S_1}, $W_{\delta'}$) calculated for different lithium concentrations (X^{α}_{Li}) in the solid solution of the cold-rolled 1420 alloy.

X^{α}_{Li}	ε, %									
	0		8		30		50		70	
	$W_{\delta'}$	W_{S_1}	$W_{\delta'}$	W_{S_1}	$W_{\delta'}$	W_{S_1}	$W_{\delta'}$	W_{S_1}	$W_{\delta'}$	W_{S_1}
0	20.9	5.4	20.9	5.4	20.4	5.9	18.9	7.4	13.8	12.4
0,1	20.1	5.3	20.1	5.3	19.6	5.8	18.1	7.3	13.0	12.3
0,2	19.3	5.1	19.3	5.1	18.8	5.6	17.3	7.1	12.1	12.2
0,4	17.7	4.7	17.7	4.7	17.1	5.3	15.5	6.8	10.2	12.1
0,5	16.8	4.6	16.8	4.6	16.3	5.1	14.7	6.7	9.2	12.0
0,6	15.9	4.4	15.9	4.4	15.4	4.9	13.7	6.5	8.2	11.9
0,7	15.0	4.2	15.0	4.2	14.5	4.7	12.8	6.4	7.2	11.8
0,8	14.1	4.0	14.1	4.0	13.5	4.5	11,8	6,2	6,2	11,7
0,9	13.1	3.8	13.1	3.8	12,5	4,3	10,8	6,0	5,1	11,6
1,0	12.1	3.6	12.1	3.6	11.5	4.1	9.8	5.8	4	11.6
1,1	11.1	3.4	11.1	3.4	10,5	3,9	8,7	5,7	2,8	11,5
1,2	10	3.1	10	3.1	9.4	3.7	7.6	5.5	1.6	11.4
1,3	9.0	2.9	9.0	2.9	8,3	3,5	6,5	5,3	0,4	11,2

'Route 1': ε = 0%: $W_{\delta'}/W_{S_1}/X^{\alpha}_{Li}$ = 12.1/3.6/1.0 → 8%: 13.1/3.8/0.9 → 30%: 13.5/4.5/0.8 → 50%: 13.7/6.5/0.6 → 70%:13.8/12.4/0.0.
'Route 2': ε = 0%: 9.0/2.9/1.3 → 8%: 11.1/3.4/1.1 → 30%: 11.5/4.1/1.0 → 50%: 12.8/6.4/0.7 → 70%:13.0/12.3/0.1.

changes in the phase composition with increasing degree of reduction showed that they lie in fairly narrow intervals (Figs. 7, *b* and 7, *c*), especially with regard to the S_1-phase content (Fig. 7, *c*). One can clearly conclude that cold rolling of the 1420 alloy in a concrete structural-phase initial state is accompanied by the decomposition of the solid solution with the precipitation of mainly S_1-phase.

At the same time, Figure 2 shows that the variation of lithium content in the solid solution can substantially affect the quantitative evaluation of the phase composition. This is especially important for the cases of heat treatment (quenching and aging), where both precipitation and dissolution of various intermetallic phases are possible along with the change of lithium content in the solid solution. In this case, it is important to know the lithium content in the solid solution of the Al–Cu(Mg)–Li alloys as a function of the alloy composition and the type of heat treatment. Such data can be obtained by comparing the calculations by the method proposed in this work and the experimental data on the lattice parameters of the solid solution for this alloy.

4. CONCLUSION

1. The method for the calculation of the T_1-, S_1- and δ′-phase contents in Al–Cu–Li and Al–Mg–Li alloys on the basis of the experimental measurement of the α-solid solution lattice parameters is proposed, where the lithium content in the solid solution serves as a variable parameter.
2. The phase relationships between the δ′-phase and the ternary phases in the Al–Cu–Li and Al–Mg–Li alloys show that the contents in the alloys with magnesium are about the same, while the δ′-phase content in the Al–Cu–Li alloys substantially exceeds the content of the ternary phase.
3. It is shown that the developed method can be effectively used for quantitative interpretation of the research data on the effect of heat and thermomechanical treatments on the phase composition of the alloys, as well as for the optimization of the Al–Mg(Cu)–Li–X alloy compositions.
4. The unusual strength anisotropy, which in the textured sheets from lithium-containing alloys substantially exceeds the anisotropy of the properties of other aluminium alloys can be due to the precipitation of the textured δ′-phase, which is similar to the texture of the solid solution, but has a specific deformation mechanism caused by the long-range ordering.
5. It is shown that the information on the quantitative ratio between intermetallic phases allows the estimation of the volume and linear changes in the alloys upon heat treatment and plastic deformation.

ACKNOWLEDGEMENTS

This work was performed in the framework of state task 11.1978.2014/K of the Ministry of Education and Science of the Russian Federation ‘Development of quantitative methods of estimating the structural phase and stressed states of Al–Cu–Li and Al–Mg–Li alloys for the feasibility and the designing of alloys and technologies providing high strength, elasticity, and phase stability characteristics of a base metal and a weld construction material’.

REFERENCES

1. V. V. Antipov, N. I. Kolobnev, and L. B. Khokhlatova, *Metallovedenie i Termicheskaya Obrabotka Metallov*, No. 9: 5 (2013) (in Russian).
2. V. V. Shestov, V. V. Antipov, O. G. Senatorova, and V. V. Sidel’nikov, *Metallovedenie i Termicheskaya Obrabotka Metallov*, No. 9: 28 (2013) (in Russian).
3. I. N. Fridlyander, K. V. Chuistov, A. L. Berezina, and N. I. Kolobnev,

Aluminium–Lithium Alloys: Structure and Properties (Kiev: Naukova Dumka: 1992) (in Russian).
4. S. Katsikis, B. Noble, and S. J. Harris, *Mater. Sci. Eng. A*, **485**: 613 (2008).
5. M. Trinca, A. Avalino, H. Garmestani, J. Foyos, E. W. Lee, and O. S. Es-Said, *Mater. Sci. Forum*, **331–337**: 849 (2000).
6. A. A. Ilyin, V. V. Zakharov, M. S. Betsofen, O. E. Osintsev, and T. A. Rostova, *Russian Metallurgy (Metally)*, No. 5: 406 (2008).
7. H. Y. Hunsicker, *Trans. AIME*, **VII**: 759 (1980).
8. S. Y. Betsofen, A. A. Ilyin, O. E. Osintsev, and M. S. Betsofen, *Russian Metallurgy (Metally)*, No. 6: 506 (2008).
9. S. Y. Betsofen, V. V. Antipov, I. A. Grushin, M. I. Knyazev, L. B. Khokhlatova, and A. A. Alekseev, *Russian Metallurgy (Metally)*, No. 1: 51 (2015).
10. W. B. Pearson, *Handbook of Lattice Spacings and Structures of Metals and Alloys* (New York: Pergamon Press: 1958).
11. Y. Ma, X. Zhou, G. E. Thompson, T. Hashimoto, P. Thomson, and M. Fowles, *Materials Chemistry and Physics*, **126**: 46 (2011).
12. Sang Yoon Park, Won Jong Choi, Heung Soap Choi, and Hyuk Kwon, *J. Mater. Process. Technol.*, **210**: 1008 (2010).
13. Po-Yu Chang and Jenn-Ming Yang, *Intern. J. Fatigue*, **30**: 2165 (2008).
14. E. P. George, D. P. Pope, C. L. Fu, and J. H. Schneibel, *ISIJ Intern.*, **31**: 1066 (1991).